Available online at www.sciencedirect.com
ScienceDirect
Catalysis Today 133–135 (2008) 267–276
CATALYSIS TODAY
www.elsevier.com/locate/cattod

Analysis of the HDS of 4,6-DMDBT in the presence of naphthalene and carbazole over NiMo/Al_2O_3–SiO_2(x) catalysts

Felipe Sánchez-Minero, Jorge Ramírez *, Aída Gutiérrez-Alejandre, César Fernández-Vargas, Pablo Torres-Mancera, Rogelio Cuevas-Garcia

UNICAT, Departamento de Ingeniería Química, Facultad de Química, UNAM, Cd. Universitaria, 04510 México, D.F., Mexico

Available online 1 February 2008

Abstract

NiMo catalysts were prepared on γ-Al_2O_3 modified with SiO_2 (0 and 10 wt% SiO_2). Catalysts were characterized by HRTEM in sulfided state and evaluated in the hydrodesulfurization (HDS) of 4,6-dimethyldibenzothiophene (4,6-DMDBT), hydrogenation (HYD) of naphthalene, hydrodenitrogenation (HDN) of carbazole and in the simultaneous reaction of 4,6-DMDBT–naphthalene–carbazole. The kinetic parameters of Langmuir–Hinshelwood type equations for all the reaction systems were estimated. Although naphthalene and carbazole present a competitive inhibition effect for the HDS of 4,6-DMDBT, the inhibiting effect of naphthalene was mainly due to its high concentration, whereas the inhibition caused by carbazole was due to its strong adsorption over the catalytic active sites. The addition of SiO_2 to the catalysts enhanced the hydrogenation activity and therefore the HDS of 4,6-DMDBT, HYD of naphthalene and HDN of carbazole leading to more active catalysts when a mixture of the three compounds was hydrotreated.

Keywords: Hydrodesulfurization; 4,6-DMDBT; Naphthalene; Carbazole; Hydrogenation; NiMo/Al_2O_3–SiO_2 catalysts; L–H equations

1. Introduction

Fossil fuels are and will be for many years more the main energy source, due to its lower cost and high efficiency in their transformation. However, due to the each time more strict environmental regulations on the sulfur content for transportation fuels, the refining industry has to make periodic changes to improve the performance of the hydrodesulfurization (HDS) catalysts. To fulfill the environmental regulations existing today, it is necessary to eliminate the most refractory sulfur compounds present in the intermediate distillates. Literature reports [1–6] indicate that the desulfurization of 4,6-dimethyldibenzothiophene (4,6-DMDBT), one of the most refractory molecules to HDS, occurs by several reaction routes like direct desulfurization (DDS), hydrogenation (HYD) and isomerization (ISOM), being the hydrogenation route the most favored [7–10]. However, this reaction pathway is strongly affected by aromatic and nitrogen compounds present in the intermediate distillates [11–13]. Recently, it has been established that nitrogen compounds of the carbazole type have an important negative influence in the performance of hydrodesulfurization catalysts [14]. Furthermore, it has been stated that the adsorption mode for carbazole compounds is similar to that of polynuclear aromatics such as naphthalene [15] and therefore it is expected that these molecules will inhibit the HDS of 4,6-DMDBT via the hydrogenation route. Some kinetic models have been proposed for the HDS of 4,6-diethyldibenzothiophene in the presence of ethylcarbazole [16], HDS of 4,6-DMDBT in the presence of aromatic compounds [17] and for the HDS of dibenzothiophene in the presence of carbazole [18]. However, real feeds to hydrotreating process present high content of aromatic and nitrogen compounds; therefore, a kinetic model including the effects of aromatics and nitrogen compounds on the HDS is needed.

To diminish the negative effect of nitrogen and aromatic compounds on the HDS of 4,6-DMDBT it is necessary to design catalysts with increased hydrogenation functionalities. It has been reported that SiO_2-supported catalysts display increased hydrogenation properties [19]. Therefore, modification of the alumina support surface with SiO_2 could be useful to increase the hydrogenation capabilities of NiMo/Al_2O_3 hydrodesulfurization catalysts. Besides, it is known

* Corresponding author. Tel.: +52 5556225349; fax: +52 5556225366.
E-mail address: jrs@servidor.unam.mx (J. Ramírez).

0920-5861/$ – see front matter © 2007 Elsevier B.V. All rights reserved.
doi:10.1016/j.cattod.2007.12.018

that the active phase–support interaction is an important variable that affects the sulfidation of the active phase [20]. A strong interaction leads to good dispersion but increases the difficulty to achieve full sulfidation of the Mo oxide phase. On the other hand, a weak interaction between the Mo precursor and the support leads to good sulfidation but at the same time to sintering and agglomeration of the active MoS_2 phase. Therefore, tuning the active phase–support interaction is of great importance to achieve proper sulfidation and dispersion of the active phase. Achieving proper sulfidation and stacking of the MoS_2 crystallites promoted by Ni or Co could lead to the formation of type NiMoS-II sites, which are more active than those with lower stacking and incomplete sulfidation [21]. For the case of hydrotreating catalysts supported on γ-Al_2O_3, the strong interaction between Mo phase and support is caused by the bonding of the Mo oxide phase to the most basic hydroxyl groups of the alumina, those bonded to aluminum in tetrahedral coordination [22–24]. In this context, surface modification with small amounts of SiO_2 will decrease the number of the most reactive hydroxyls groups on the surface of the alumina support, which will allow an easier sulfidation of the Ni and Mo supported phases. Amorphous silica–alumina (ASA) supports present an acidic nature [25]. Although literature reports indicate that acidity can improve the HDS reaction [26,27], the impregnation of SiO_2 on the surface of alumina might display the same behavior.

The aim of the present work is to determine the effect of silica incorporation to the alumina support when preparing $NiMo/Al_2O_3$–$SiO_2(x)$ catalysts for the hydrotreatment of mixtures of 4,6-DMDBT–naphthalene–carbazole. The synthesized catalysts were evaluated in the HDS of 4,6-DMDBT, HYD of naphthalene, hydrodenitrogenation (HDN) of carbazole, and in the simultaneous reaction of 4,6-DMDBT–naphthalene–carbazole. From the fit of the experimental results to Langmuir–Hinshelwood (L–H) type equations, reaction rate and adsorption constants were evaluated for the transformation of the single reactants and their mixture. The quantitative estimation of the reaction rate and adsorption constants provides information on the strength of carbazole and naphthalene inhibition, which is useful for the design of catalytic hydrodesulfurization systems. Besides, catalytic samples were characterized by nitrogen physisorption, FTIR pyridine adsorption and hydroxyl region. The dispersion of sulfided catalysts was analyzed by high-resolution transmission electron microscopy (HRTEM).

2. Experimental

2.1. Supports and catalysts preparation

Commercial γ-Al_2O_3 was surface modified with SiO_2 using the following procedure: tetraethylorthosilicate (TEOS) of 99.5 wt% purity was slowly added to a suspension of γ-Al_2O_3 in anhydrous ethanol in order to obtain the required SiO_2 wt%. The suspension was agitated at 351 K during 12 h. After that, the support was filtered under vacuum, then dried at 373 K for 24 h and finally calcined at 823 K for 4 h. Supports were labeled as SAC *X*, where *X* represents the wt% SiO_2 (0 and 10%).

NiMo–SAC catalysts were synthesized by successive impregnation (pore volume method) of Mo and Ni, respectively. First, aqueous solution of ammonium heptamolybdate was used in appropriate amounts to obtain a concentration of 2.8 Mo atoms/nm^2. Mo-SAC catalysts were dried at 373 K and calcined at 773 K during 3 h. Then, an aqueous solution of nickel nitrate was used in appropriate amounts of Ni to obtain the ratio Ni/(Ni + Mo) = 0.3. NiMo–SAC catalysts were dried at 373 K and calcined at 773 K during 3 h. Here after, the catalysts will be labeled NiMo–SAC *X*, where *X* represents the wt% of SiO_2 in the support.

2.2. Characterization

The textural properties of supports and catalysts were evaluated by N_2 physisorption using a Micromeritics ASAP 2000 apparatus. Before measurements, the samples were outgassed at 543 K under vacuum during 4 h.

For the FTIR analysis in the hydroxyl region, a thin wafer of pure powders (8 mg/cm^2) placed into a special IR cell was pretreated under vacuum at 773 K for 1 h. After that, the IR spectrum was collected. For pyridine adsorption experiments, samples were pretreated under oxygen atmosphere at 723 K during 12 h and then under vacuum for 2 h at 723 K. After that, a pulse of pyridine was introduced at room temperature and IR spectra were collected outgassing at room temperatures 373, 473 and 573 K. Experiments were performed with a Nicolet Magna 760 FTIR spectrometer using 100 scans and a resolution of 2 cm^{-1}.

Sulfided catalysts were characterized by HRTEM using a JEOL 2010 microscope with a 1.9 Å point-to-point resolution.

2.3. Catalytic activity

The reaction experiments were conducted in batch reactor operating at 1200 psi and 598 K, the catalysts were presulfided ''ex situ'' in a continuous flow reactor operating at atmospheric pressure and 673 K for 4 h using a 15% H_2S/H_2 gas mixture. In each reaction tests, the batch reactor was loaded with 200 mg of catalyst with 40 ml of a mixture containing the reactants. For the HDS tests, a solution containing 1000 ppm of S as 4,6-DMDBT was used. For HYD tests, a solution of 5 wt% naphthalene was used. For HDN tests, a solution with 100 ppm of N as carbazole was used. For the tests using the three reactants, the used solution contains 1000 ppm of S as 4,6-DMDBT, 5 wt% naphthalene and 100 ppm of N as carbazole. The solvent used for all the tests was a 70/30 wt% mixture of *n*-decane/*m*-xylene. The reactivity of this solvent was also evaluated.

Analysis of the reaction products was performed with an HP 6890 chromatograph. Additionally, reaction products were identified by GC–mass spectrometry.

Table 1
Supports and catalysts textural properties

Sample	BET surface area (m^2/g)	Pore volume (cm^3/g)	Average pore diameter (nm)
SAC 0.0	242	0.50	6.76
SAC 10.0	223	0.47	6.59
NiMo–SAC 0.0	206	0.39	6.38
NiMo–SAC 10.0	176	0.34	6.27

3. Results and discussion

3.1. Characterization

3.1.1. Nitrogen physisorption

Table 1 shows the BET surface area for supports and catalysts. The impregnation of 10 wt% silica to the alumina support only caused a slight decrease in surface area. Similar results were obtained after molybdenum and nickel impregnation. The pore size distribution curves (not shown) presented monomodal distribution. A small decrease in pore volume and average pore size was observed when silica, molybdenum and nickel were added.

3.1.2. FTIR hydroxyl region

To assess the elimination of the most basic hydroxyl groups bonded to tetrahedral aluminum when silica is incorporated to alumina, infrared analysis of the hydroxyl region was performed. Fig. 1 shows the IR spectra of SAC supports in the hydroxyl-stretching region. The IR spectrum of SAC 0 (alumina) present the characteristic bands of Al_2O_3 hydroxyl groups at 3790, 3775, 3740, 3730 and 3680 cm^{-1} [22–24]. According to Knözinger and Ratnasamy [24], the most basic hydroxyl groups in alumina give rise to an IR band at 3775 cm^{-1}. For our study, this band is well evident. When silica is incorporated to alumina (SAC 10), some changes in the bands intensity are observed. A new band localized in the region at 3725–3750 cm^{-1} appears. This band is assigned to isolated silanol groups [28,29]. Besides, the band corresponding to the most basic hydroxyl groups (3775 cm^{-1}) disappear. This behavior indicates that at the silica content of 10 wt% complete elimination of the most basic hydroxyl groups in alumina. Therefore, for this catalyst formulation the interaction between the Mo oxide phase and the support is expected to decrease.

3.1.3. FTIR pyridine adsorption

To enquire about the changes in the support acidity when SiO_2 is added, experiments of pyridine adsorption were performed. According to literature reports [30], the bands at 1460–1445 and 1600–1633 cm^{-1} are assigned to the υ_{8a} and υ_{19b} vibration modes of chemisorbed pyridine on coordinative unsaturated Al^{3+} sites (Lewis sites). The bands at 1500–1540 and 1630–1640 cm^{-1} are typical of the υ_{8a} and υ_{19b} vibration modes of adsorbed pyridinium species (Brønsted sites).

Fig. 2 shows the IR spectra of chemisorbed pyridine on SAC supports. For SAC 0, we mainly observed the presence of strong IR bands assigned to Lewis acid sites: one at 1450 cm^{-1} and another with two maxima at 1614 and 1622 cm^{-1}. The vibration of the υ_{8a} mode of pyridine molecules at two different frequencies (1614 and 1622 cm^{-1}) indicates the presence of Lewis acid sites with different strength [31]. These sites can be assigned to the presence of Al^{3+} Lewis sites in octahedral and tetrahedral environments, respectively.

When silica is incorporated onto alumina, there are some evident changes in number and intensity of the infrared bands assigned to Lewis acidic sites. The υ_{8a} band (1600–1633 cm^{-1}) is no longer splitted indicating the presence on surface of Al^{3+} CUS with only one coordination. The position of the band at 1615 cm^{-1} suggests pyridine chemisorbed on CUS of Al^{3+} in octahedral coordination. The intensity of the bands at 1615 and 1450 cm^{-1} decreases with the addition of silica, suggesting a small decrease in the number of Lewis acid sites, possibly those covered by the silica addition.

Therefore, the incorporation of silica to alumina did not increase significantly the Brønsted acidity of the sample. This is possibly due to the fact that contrary to typical ASA supports where silica is incorporated to the bulk structure [25]. In our study, silica was deposited on the external surface of alumina without formation of strong Al–OH–Si Brønsted sites. This behavior has been reported in the past for similar samples by Finocchio et al. [32].

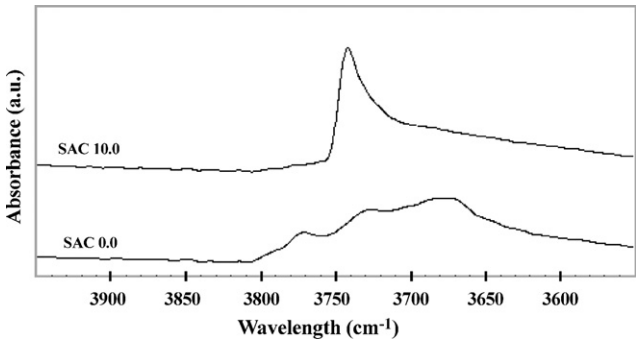

Fig. 1. FTIR spectra of supports in the hydroxyl region, after outgassing at 773 K during 1 h.

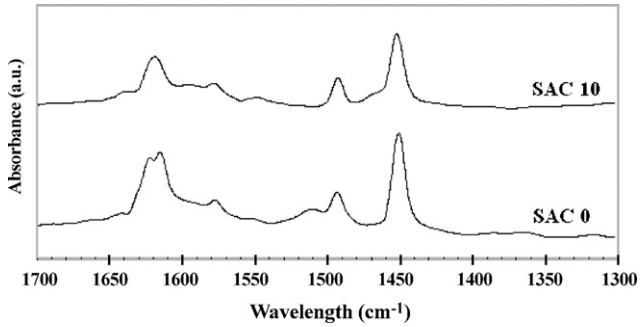

Fig. 2. FTIR spectra of supports with chemisorbed pyridine after outgassing at 373 K.

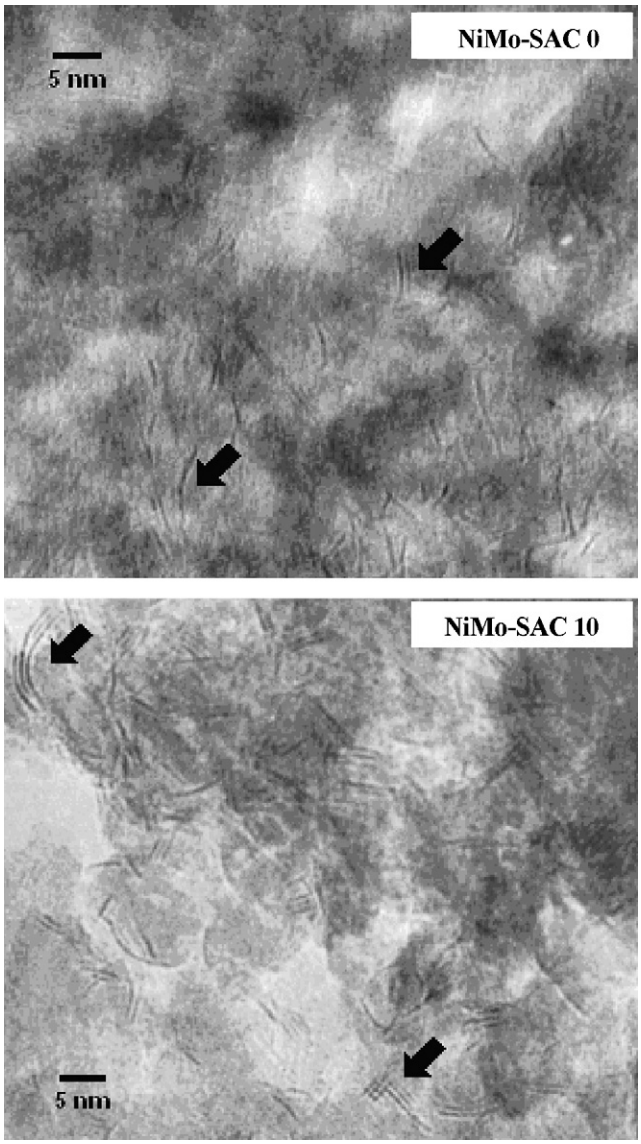

Fig. 3. HREM micrographs for NiMo–SAC 0 and NiMo–SAC 10 catalysts.

3.1.4. High-resolution transmission electron microscopy

Fig. 3 shows micrographs of the sulfided NiMo–SAC catalysts. For NiMo–SAC 0, the presence of homogeneously dispersed MoS_2 crystallites with one layer is observed. In contrast, NiMo–SAC 10 presents highly stacked MoS_2 crystallites.

Statistical analysis of the length and stacking of the crystallites (see Fig. 4) shows that although the length distribution of MoS_2 crystallites is similar for both catalysts (~3.2 nm average crystallite length); the stacking of the crystallites is enhanced when silica is incorporated to alumina support. NiMo–SAC 10 presents an average number of layers of 2.3 compared to 1.5 displayed by NiMo–SAC 0. The higher stacking of the MoS_2 crystallites on NiMo–SAC 10 seems to be the result of the lower interaction between the active phase and the support. It is expected that the higher stacking of NiMo–SAC 10 will favor the hydrogenation of aromatic rings, which interact during reaction with more than one coordinatively unsaturated Mo site.

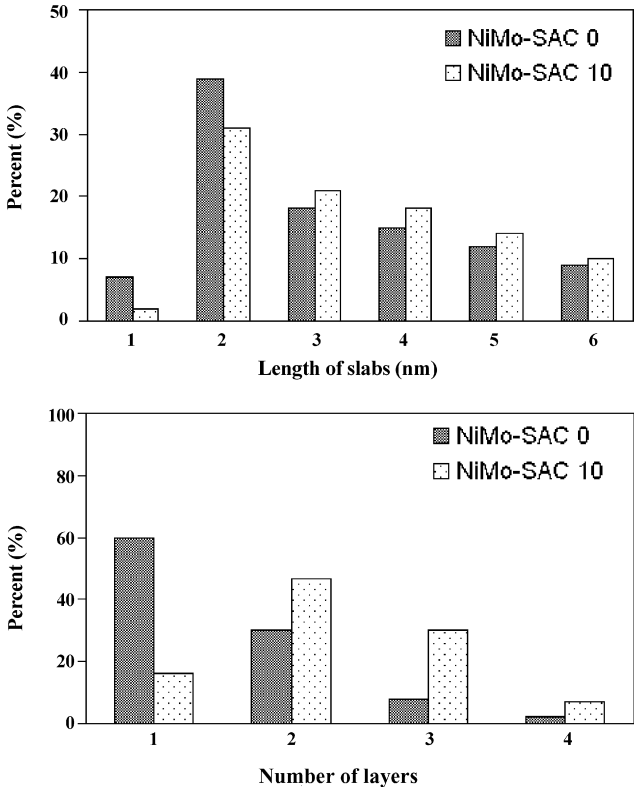

Fig. 4. Crystal size distribution of MoS_2 for sulfided NiMo–SAC catalysts.

3.2. Catalytic activity

3.2.1. Solvent reactivity

The use of a mixture *n*-decane/*m*-xylene (70/30 wt%) was necessary to allow the dissolution at carbazole, which is practically insoluble in pure *n*-decane. To evaluate the effect of the solvent *n*-decane/*m*-xylene during the reactions a catalytic test without the main reactants was performed using the NiMo–SAC 0 and NiMo–SAC 10 catalysts. Results showed no significant conversion of decane to cracking products and only a small hydrogenation of *m*-xylene (less than 5% conversion after 4 h of reaction time) as shown in Fig. 5. As a result, the contribution of the solvent in the kinetic study was neglected.

To help the interpretation of results, simplified reaction schemes for the hydrodesulfurization of 4,6-DMDBT, hydrogenation of naphthalene and hydrodenitrogenation of carbazole are shown in Scheme 1.

3.2.2. 4,6-DMDBT hydrodesulfurization

Fig. 6 shows a comparison of the 4,6-DMDBT HDS conversion as a function of the reaction time for NiMo–SAC 0 and NiMo–SAC 10. After 4 h reaction time NiMo–SAC 10 reaches a conversion of nearly 80% compared to 67% displayed by the NiMo–SAC 0. Although both catalysts present a similar acidity, the increase in the activity when NiMo–SAC 10 is used may be related with its increase in the number of layers of MoS_2 crystallites, since this favors the adsorption of the molecules of 4,6-DMDBT through the π aromatic system.

Fig. 7 shows a plot of the yield of each product versus the conversion of 4,6-DMDBT. It is known that HDS of 4,6-

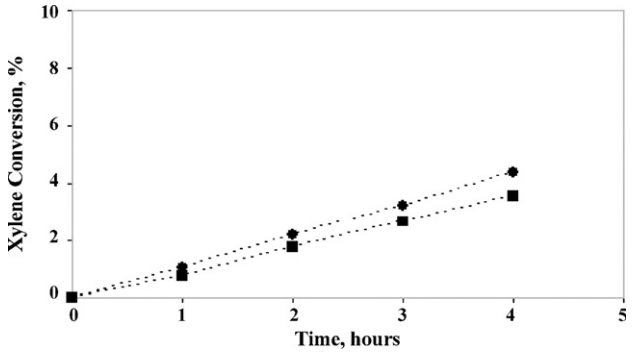

Fig. 5. Xylene conversion for NiMo–SAC 0 (■) and NiMo–SAC 10 (●) catalysts.

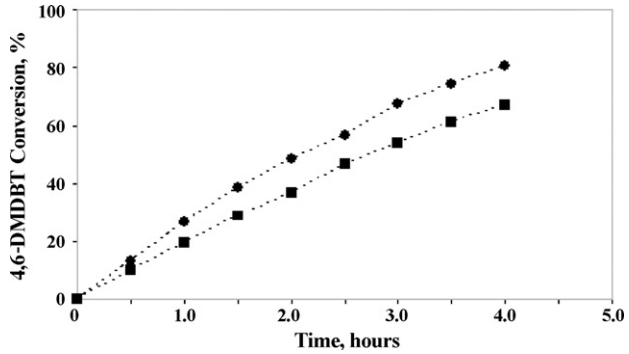

Fig. 6. 4,6-DMDBT conversion for NiMo–SAC 0 (■) and NiMo–SAC 10 (●) catalysts.

DMDBT takes place by several reaction routes (see Scheme 1a): direct desulfurization, hydrogenation and isomerization [1–6]. However, in our case no products from the isomerization route were detected. In the tests, the main product was methylcyclohexyltoluene (MCHT), which comes from the hydrogenation of 4,6-DMDBT followed by desulfurization. The final yields for this product after 4 h reaction time were 47 and 55% for NiMo–SAC 0 and NiMo–SAC 10, respectively. Indicating an increase in the hydrogenation activity when silica this present in the catalyst. The contribution of the direct desulfurization route to the formation of dimethyldiphenyl (DMDP) was minor and similar for both catalysts (∼9% yield). Indicating that the addition of silica to the surface at alumina does not affect significantly this route of reaction presumably because the surface acidity is not considerably modified. Other product detected in the reaction mixture was dimethyldicyclohexyl, which comes mainly from the consecutive hydrogenation of MCHT. The slightly higher yield of DMDCH obtained with the NiMo–SAC 10 catalyst is in agreement with the higher hydrogenation activity of the silica-modified

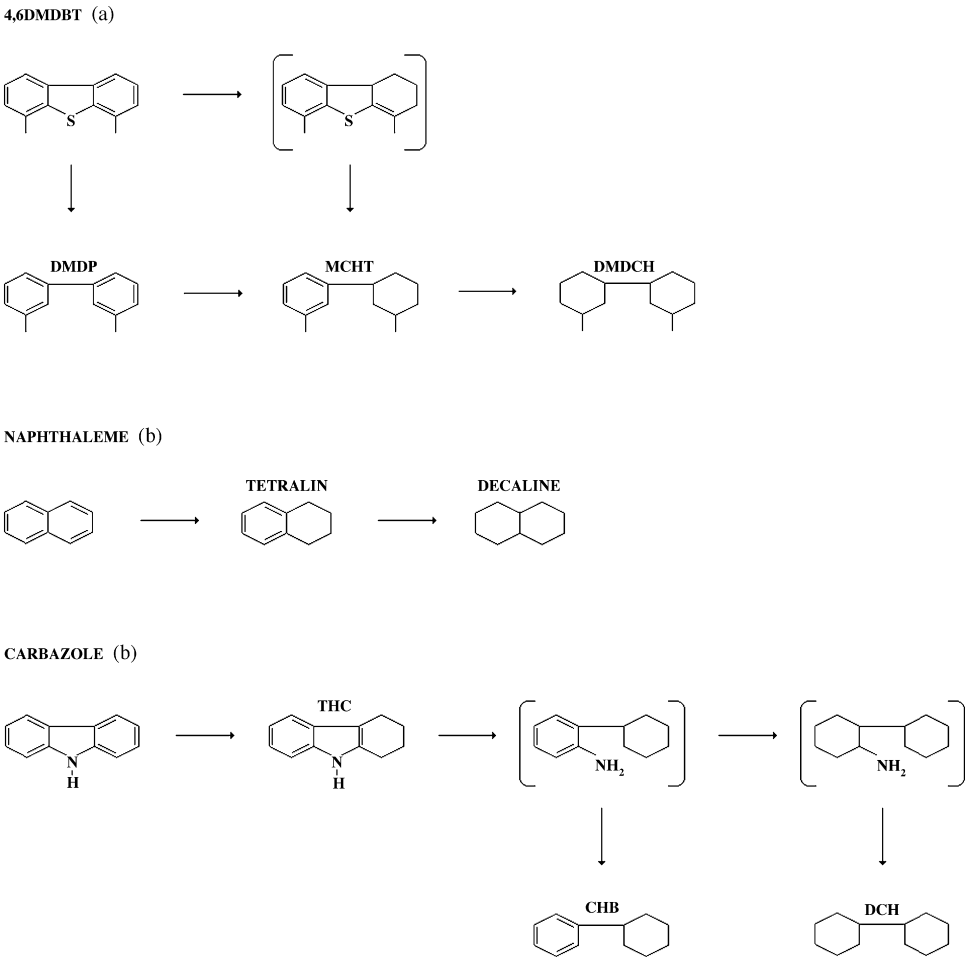

Scheme 1. Simplified reaction scheme for 4,6-DMDBT (a), naphthalene (b) and carbazole (c).

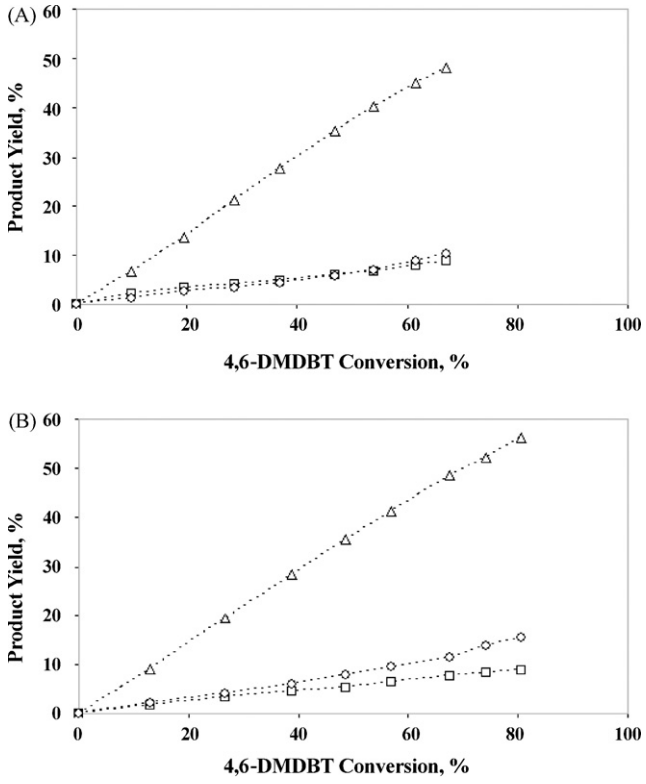

Fig. 7. Products distribution for 4,6-DMDBT hydrodesulfurization: (□) DMDP, (△) MCHT and (○) DMDCH for NiMo–SAC 0 (A) and NiMo–SAC 10 (B) catalysts.

catalyst. The above results clearly indicate that the transformation of 4,6-DMDBT occurs through the hydrogenation reaction route and that this route is enhanced by the addition of silica to the alumina support.

Although small quantities of DMDP are hydrogenated, the higher values of the ((MCHT + DMDCH)/DMDP) ratio displayed by the NiMo–SAC 10 catalyst (Fig. 8) corroborate the enhanced selectivity towards hydrogenation of this catalyst.

3.2.3. Naphthalene hydrogenation

In agreement with the results from the HDS of 4,6-DMDBT, Fig. 9 shows that when the silica is present in the catalyst increases so does the hydrogenation of naphthalene. After 2.5 h reaction time NiMo–SAC 10 reaches a conversion of nearly 93% compared to 88% displayed by the catalyst NiMo–SAC 0.

Although tetralin was identified as the main reaction product for both catalysts (82–85% yield after 2.5 h reaction time), the yield of decalines increases slightly when silica is present in the support, indicating according to Scheme 1b better hydrogenation of the second naphthalene ring (Fig. 10). The final yields for this product were 6 and 8% for NiMo–SAC 0 and NiMo–SAC 10, respectively. Products derived from ring breaking were not observed in the reaction products for NiMo–SAC catalysts. Analysis of the decalines for both catalysts shows that the *trans*-decaline this present in more quantity that the *cis*-decaline, besides, *trans*/*cis*-decaline ratio remains constant. This indicates that the acidity at the catalyst does not increase significantly with silica addition since the *trans*/*cis*-decaline ratio normally increases with catalyst acidity [33].

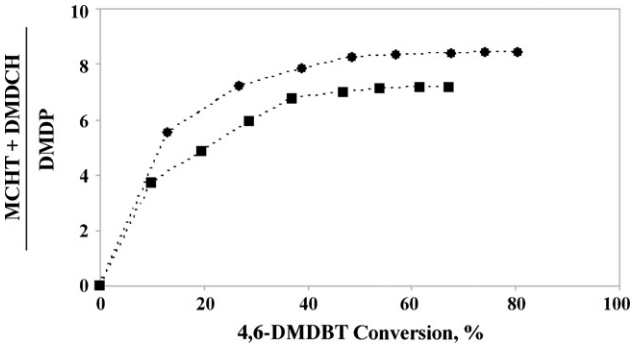

Fig. 8. HYD/DDS ratio vs. 4,6-DMDBT conversion, for NiMo–SAC 0 (■) and NiMo–SAC 10 (●) catalysts.

3.2.4. Carbazole hydrodenitrogenation

The results of carbazole HDN show that NiMo–SAC 10 is more active that NiMo–SAC 0 (see Fig. 11). The conversion of carbazole after 2.5 h reaction time is 79% for NiMo–SAC 0 and 88% for NiMo–SAC 10. This increase in the activity corroborate the improve in the hydrogenation capacity when silica is present in the catalyst since carbazole HDN reaction is favored for this route [34].

According to the literature [34,35], the carbazole HDN has two possible reaction pathways; the direct denitrogenation route (DDN), which leads to diphenyl (DP) as the main product and the hydrogenation route that leads to tetrahydrocarbazole (THC) as intermediate product, and then to cyclohexylbenzene (CHB) and dicyclohexyl (DHC) as final products (Scheme 1c). Fig. 12 revealed that the product of DDN route was absent and that the main product of reaction was cyclohexylbenzene. The final yields for this product after 2.5 h reaction time were 43 and 49% for NiMo–SAC 0 and NiMo–SAC 10, respectively. Although the main product was the CHB, an increase in the DCH content is clearly observed when SiO_2 is present in the catalyst. THC was observed principally when NiMo–SAC 0 catalyst is used. This indicates that catalyst without silica content has problems to transform the THC into its hydrogenation products.

3.2.5. HDS of 4,6-DMDBT in the presence of naphthalene and carbazole

Conversion results of 4,6-DMDBT in the presence of naphthalene and carbazole are presented in Fig. 13. NiMo–SAC

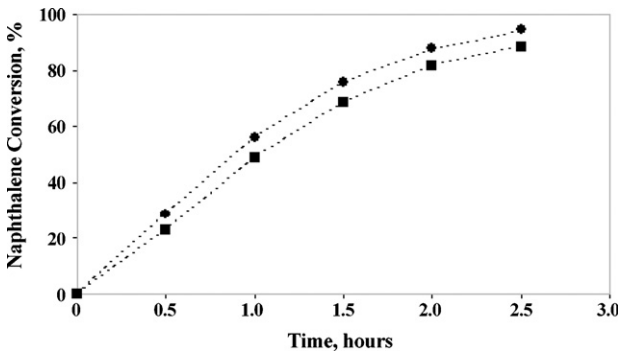

Fig. 9. Naphthalene conversion for NiMo–SAC 0 (■) and NiMo–SAC 10 (●) catalysts.

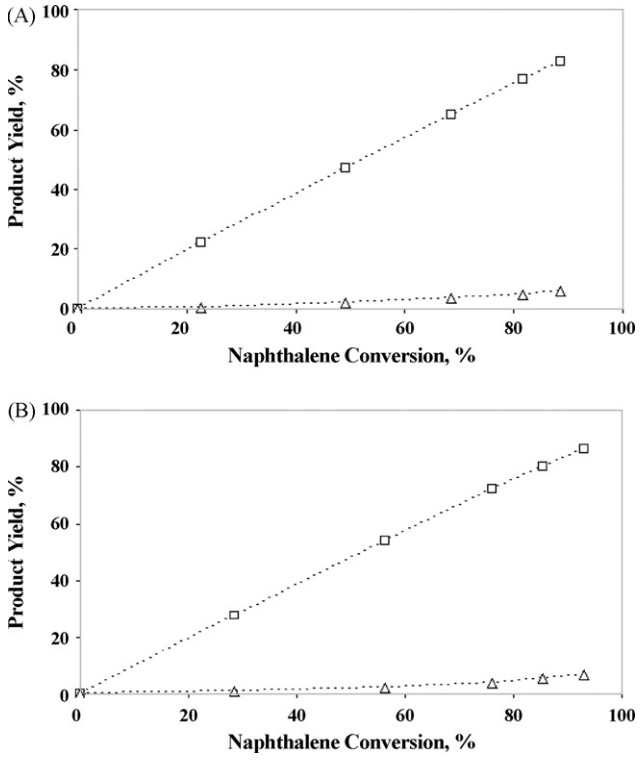

Fig. 10. Products distribution for naphthalene hydrogenation: (□) tetraline and (△) decaline for NiMo–SAC 0 (A) and NiMo–SAC 10 (B) catalysts.

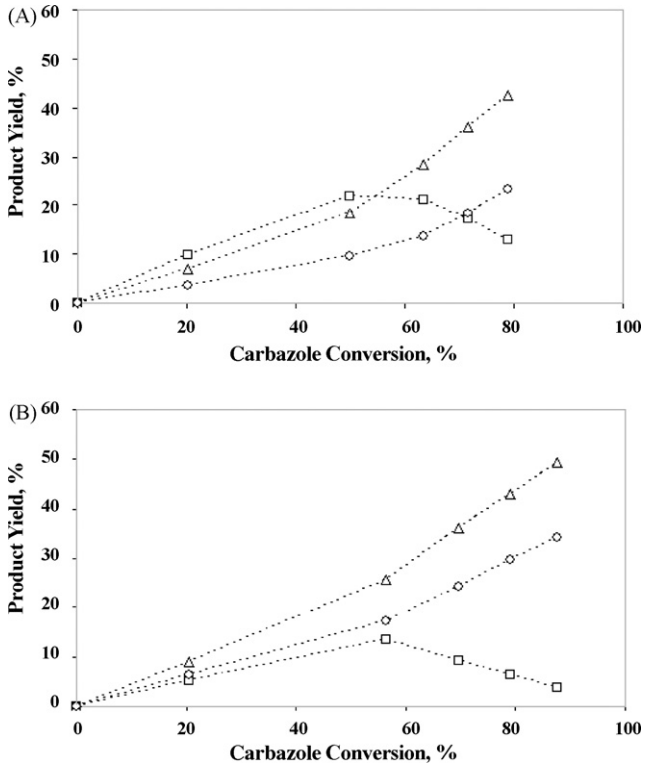

Fig. 12. Products distribution for carbazole hydrodenitrogenation: (□) THC, (△) CHB and (○) DCH for NiMo–SAC 0 (A) and NiMo–SAC 10 (B) catalysts.

10 catalyst continues maintaining more activity than NiMo–SAC 0 because all the compounds react through the hydrogenation route.

Comparing the HDS of 4,6 DMDBT with simultaneous HDS–HYD–HDN test several effects were observed: (i) a decrease in the HDS activity when naphthalene and carbazole were added, (ii) the shape of the 4,6-DMDBT conversion curve versus time changed from concave (HDS of 4,6-DMDBT) to convex (HDS of 4,6-DMDBT in the presence of naphthalene and carbazole) and (iii) after high naphthalene conversion is reached and THC begins to react the conversion rate of 4.6-DMDBT increases. The inhibition effects observed for the HDS of 4,6-DMDBT when naphthalene and carbazole are present in the mixture needs a kinetic study to be explained.

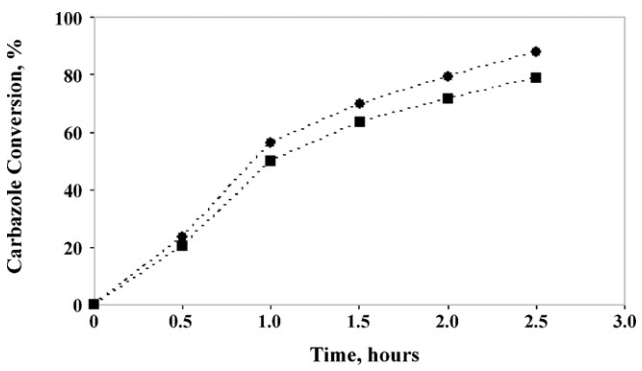

Fig. 11. Carbazole conversion for NiMo–SAC 0 (■) and NiMo–SAC 10 (●) catalysts.

3.3. Kinetic study

A kinetic study for each one of the reactions (4,6-DMDBT, naphthalene and carbazole) was carried out. For this study, a Langmuir–Hinshelwood (L–H) type equation was used. Besides, following aspects were considered: irreversible reactions, the effect at hydrogenated products concentration was neglected, since hydrogen is in excess its concentration remains constant through the reaction and therefore a pseudo zero order was considered. Table 2 presents the estimated kinetic parameters of the L–H mechanisms that presented the best fit.

3.3.1. 4,6-DMDBT hydrodesulfurization

L–H type equation with two active sites presented a high correlation (Fig. 14a). Previously, Broderick and Gates [36] and

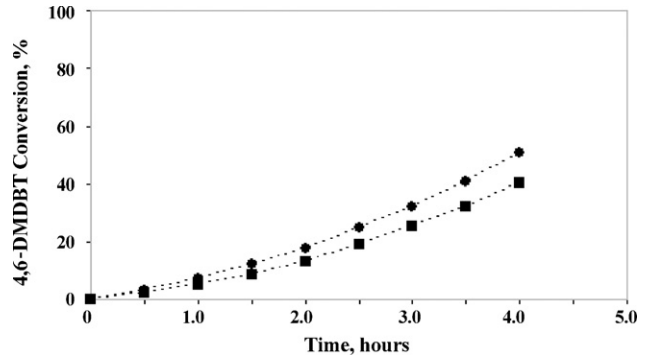

Fig. 13. 4,6-DMDBT conversion in the presence of naphthalene (5.0 wt%) and carbazole (0.01 wt% nitrogen) for NiMo–SAC 0 (■) and NiMo–SAC 10 (●) catalysts.

Table 2
Reaction rate and adsorption constants for 4,6-DMDBT HDS, naphthalene HYD and carbazole HDN

Catalyst	k (h^{-1})	K_A (L/mol)	R^2	L–H equation
4,6-DMDBT hydrodesulfurization				
NiMo–SAC 0	1.3731	9.2685	0.9969	$-\frac{dC_{46}}{dt}=\frac{kC_{46}}{(1+K_AC_{46})^2}$
NiMo–SAC 10	1.6805	9.6805	0.9996	
Naphthalene hydrogenation				
NiMo–SAC 0	1.3463	3.9093	0.9977	$-\frac{dC_N}{dt}=\frac{kC_N}{1+K_AC_N}$
NiMo–SAC 10	1.4686	3.3747	0.9883	
Carbazole hydrodenitrogenation				
NiMo–SAC 0	0.7070	84.7861	0.9910	$-\frac{dC_C}{dt}=\frac{kC_C}{1+K_AC_C}$
NiMo–SAC 10	1.0728	113.8934	0.9862	

Vrinat and de Mourgues [37] reported a similar equation of type L–H for hydrodesulfurization of dibenzothiophene in the presence of H_2S formed in the reaction. The values of the kinetic parameters show an increase in the value of the reaction rate constant (k_{46}) when NiMo–SAC 10 was used, corroborating the higher activity of this catalyst. On the other hand, the values of the adsorption constants for both catalysts are similar (~9.4 L/mol).

3.3.2. Naphthalene hydrogenation

For this study, an L–H type equation for naphthalene hydrogenation over Ni/Al_2O_3 previously reported by Rautanen et al. [38] was used. This equation presents a high correlation (Fig. 14b). In agreement with kinetic study of 4,6-DMDBT, the reaction rate constant (k_N) is slightly greater for NiMo–SAC 10.

3.3.3. Carbazole hydrodenitrogenation

For this study, L–H equation that presents higher correlation is identical to the established one for the naphthalene hydrogenation (Fig. 14c). This equation is consistent with L–H type equation proposed by Laredo et al. [18]. Although the values of the reaction rate constant (k_C) present the same tendency observed in the previous studies, the adsorption constant present a high value for both catalysts (84–114 L/mol). This explains the role of carbazole adsorption over active sites. In concordance with Szymanska studies [24], we found that carbazole is strongly adsorbed on the catalytic surface.

3.3.4. HDS of 4,6-DMDBT in the presence of naphthalene and carbazole

For the HDS of 4,6-DMDBT in the presence of naphthalene and carbazole an L–H type equation is obtained. The values of the adsorption constants obtained in the experiments with the pure compounds were used in this study. Table 3 presents the value of the kinetic parameters and the L–H equation with best fitted for the experimental results.

Table 3
Reaction rate constant for 4,6-DMDBT HDS in the presence of naphthalene and carbazole

Catalyst	k (h^{-1})	R^2	L–H equation
NiMo–SAC 0	0.4490	0.9967	$-\frac{dC_{46}}{dt}=\frac{kC_{46}}{(1+K_{A46}C_{46}+K_{AN}C_N+K_{AC}C_C)^2}$
NiMo–SAC 10	0.5206	0.9944	

Naphthalene hydrogenation (5.00 wt%) and carbazole hydrodenitrogenation (0.01 wt% nitrogen).

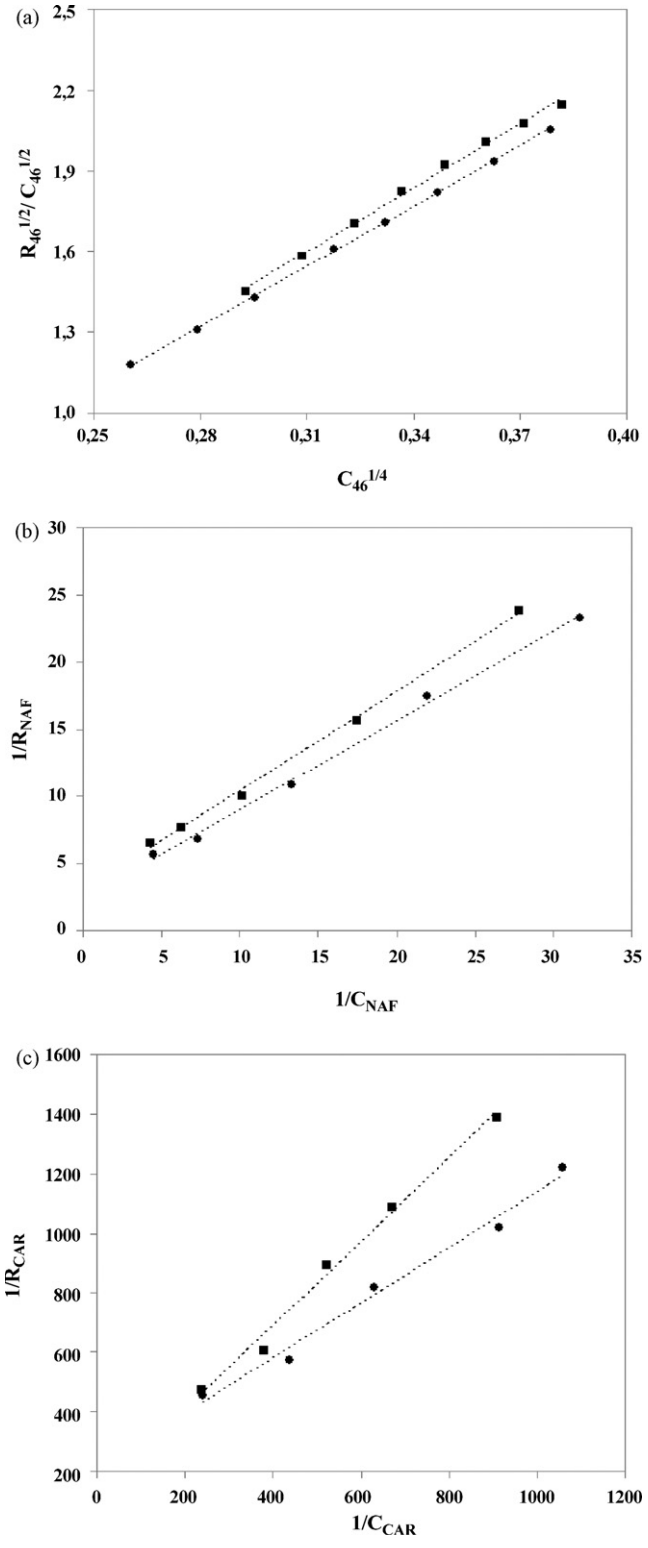

Fig. 14. Pseudo-first-order kinetics of 4,6-DMDBT HDS (a), naphthalene HYD (b) and carbazole HDN (c) for NiMo–SAC 0 (■) and NiMo–SAC 10 (●) catalysts.

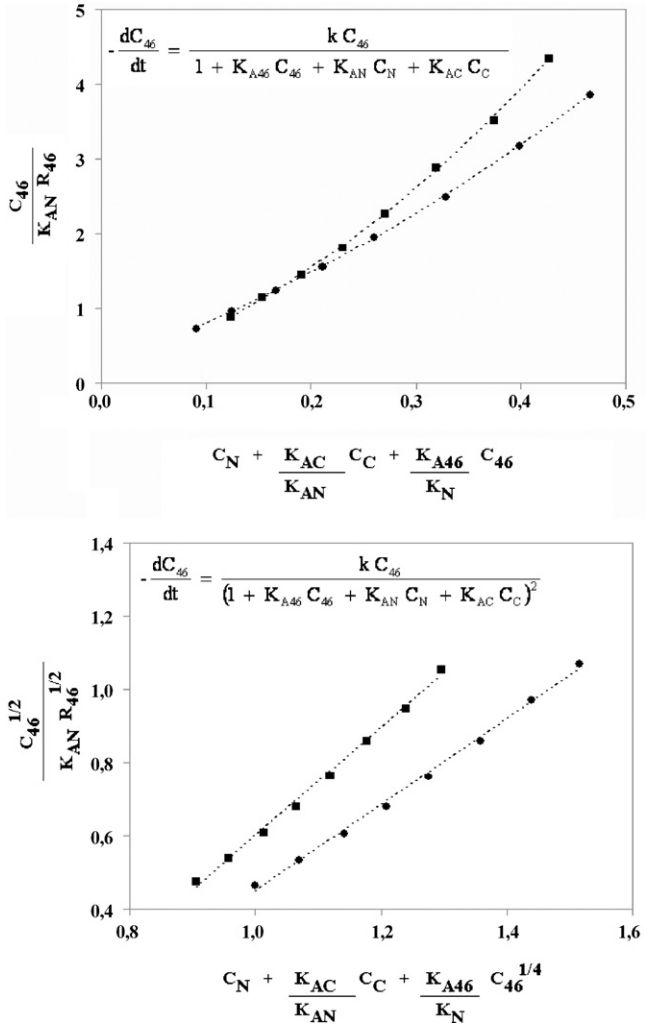

Fig. 15. L–H type equations for 4,6-DMDBT HDS in the presence of naphthalene and carbazole for NiMo–SAC 0 (■) and NiMo–SAC 10 (●) catalysts.

The estimated values of the reaction rate constants (k_{46}) for NiMo–SAC 0 and NiMo–SAC 10 are smaller compared to those obtained in the absence of naphthalene and carbazole. This corroborates the loss at activity when naphthalene and carbazole are present.

Kinetic study showed that HDS of 4,6-DMDBT is affected by the presence of naphthalene and carbazole. The values of the kinetic rate and adsorption constants indicate that the inhibition effect at naphthalene is mainly due to its high initial concentration in the mixture ($C_{0\ N} = 13C_{0\ 4,6} = 60C_{0\ C}$), so, the product $K_{AN}\ C_N$ located in the denominator of the rate equation will become negligible only after significant naphthalene conversion. For this case, the active sites can be regenerated after naphthalene reaches a high conversion (∼60%). In contrast, although carbazole present a low concentration, it adsorbs strongly on the catalytic surface. Therefore, the inhibition effect of this compound is due to the high value of the adsorption constant ($K_{AC} \sim 95$ L/mol, $K_{A4,6} \sim 9.5$ L/mol, $K_{AN} \sim 3.5$ L/mol). The $K_{AC}/K_{A4,6}$ ratio is nearly to 10, similar results were reported by Koltai et al. [17].

Fig. 15 shows the fit to the experimental results obtained with single and dual active sites L–H mechanisms. Kinetic equation with two active sites for the 4,6-DMDBT adsorption in the presence of naphthalene and carbazole presented the higher correlation.

4. Conclusions

Incorporating SiO_2 to Al_2O_3 causes the elimination of the surface hydroxyl groups most basic bonded to tetrahedral aluminum (IR band at 3775 cm^{-1}). Therefore, sulfided NiMo–SAC10 catalyst showed stacked MoS_2 crystallites with more than two layers. These sites favor the hydrogenation route, being more active for 4,6-DMDBT HDS, naphthalene HYD and carbazole HDN.

Small amounts of carbazole strongly inhibit the 4,6-DMDBT HDS reaction due to the high value of the carbazole adsorption constant with respect to 4,6-DMDBT. In contrast, naphthalene with a small adsorption constant inhibits the 4,6-DMDBT HDS reaction due to the high concentration of this aromatic in the reaction mixture.

Acknowledgments

The authors are grateful for the financial support through IN-141138 DGAPA-UNAM project. Thanks to Iván Puente Lee for HREM works. C.F.-V., P.T.-M. and F.S.-M. thank CONACyT for their Ph.D. fellowship.

References

[1] P.T. Vasudevan, J.L.G. Fierro, Catal. Rev. Sci. Eng. 38 (1996) 161.
[2] M.V. Landau, D. Berger, M. Herskowitz, J. Catal. 159 (1996) 236.
[3] K.G. Knudsen, B.H. Cooper, H. Topsøe, Appl. Catal. A 189 (1999) 205.
[4] T. Kabe, Y. Aoyama, D. Wang, A. Ishihara, W. Qian, M. Hosoya, Q. Zhang, Appl. Catal. A 209 (2001) 237.
[5] G. Pérot, Catal. Today 86 (2003) 111.
[6] D. Zuo, D. Li, H. Nie, Y. Shi, M. Lacroix, M. Vrinat, J. Mol. Catal. A 211 (2004) 179.
[7] P. Michaud, J.L. Lemberton, G. Pérot, Appl. Catal. A 169 (1998) 343.
[8] F. Bataille, J.L. Lemberton, P. Michaud, G. Pérot, M. Vrinat, M. Lemaire, E. Schulz, M. Breysse, S. Kasztelan, J. Catal. 191 (2000) 409.
[9] H. Kim, J.J. Lee, S.H. Moon, Appl. Catal. B 44 (2003) 287.
[10] M. Egorova, R. Prins, J. Catal. 225 (2004) 417.
[11] T. Isoda, S. Nagao, X. Ma, Y. Korai, I. Mochida, Appl. Catal. A 150 (1997) 1.
[12] E. Lecrenay, K. Sakanishi, I. Mochida, T. Suzuka, Appl. Catal. A 175 (1998) 237.
[13] M. Egorova, R. Prins, J. Catal. 224 (2004) 278.
[14] S. Djangkung Sumbogo Murti, H. Yang, K.-H. Choi, Y. Korai, I. Mochida, Appl. Catal. A 252 (2003) 331.
[15] T.C. Ho, J. Catal. 219 (2003) 442.
[16] T.C. Ho, D. Nguyen, J. Catal. 222 (2004) 450.
[17] T. Koltai, M. Macaud, A. Guevara, E. Schulz, M. Lemaire, R. Bacaud, M. Vrinat, Appl. Catal. A 231 (2002) 253.
[18] G.C. Laredo, A. Montesinos, J. Antonio De los Reyes, Appl. Catal. A 265 (2004) 171.
[19] B. Pawelec, R.M. Navarro, J.M. Campos-Martin, A. Lopez Agudo, P.T. Vasudevan, J.L.G. Fierro, Catal. Today 86 (2003) 73.
[20] N. Kunisada, K.-K. Choi, Y. Korai, I. Mochida, K. Nakano, Appl. Catal. A 273 (2004) 287.
[21] J.V. Lauritsen, M. Nyberg, J.K. Nørskov, B.S. Clausen, H. Topsøe, E. Laegsgaard, F. Besenbacher, J. Catal. 224 (2004) 94.
[22] N. Katada, T. Fujii, K. Iwata, Y. Hibino, M. Niwa, J. Catal. 186 (1999) 478.

[23] M. Digne, P. Sautet, P. Raybaud, P. Euzen, H. Toulhoat, J. Catal. 211 (2002) 1.
[24] H. Knözinger, P. Ratnasamy, Catal. Rev. 17 (2005) 31.
[25] S. Rajagopal, J.A. Marzari, R. Miranda, J. Catal. 151 (1995) 192.
[26] M.V. Landau, Catal. Today 36 (1997) 393.
[27] C. Kwak, M. Young Kim, K. Choi, S. Heup Moon, Appl. Catal. A 185 (1999) 19.
[28] D. Bianchini, J. Henrique Zimnoch dos Santos, T. Uozumi, T. Sano, J. Mol. Catal. A 185 (2002) 223.
[29] P. Shah, A.V. Ramaswamy, K. Lazar, V. Ramaswamy, Appl. Catal. A 273 (2004) 239.
[30] G. Busca, Catal. Today 41 (1998) 191.
[31] M. Trombetta, G. Busca, S. Rossini, V. Piccoli, U. Cornaro, A. Guercio, R. Catani, R.J. Willey, J. Catal. 179 (1998) 581.
[32] E. Finocchio, G. Busca, S. Rossini, U. Cornaro, V. Piccoli, R. Miglio, Catal. Today 33 (1997) 335.
[33] K.-C. Park, D.-J. Yim, S.-K. Ihm, Catal. Today 74 (2002) 281.
[34] A. Szymanska, M. Lewandowski, C. Sayag, G. Djega-Mariadassou, J. Catal. 218 (2003) 24.
[35] M. Nagai, Y. Goto, A. Irisawa, S. Omi, J. Catal. 191 (2000) 128–137.
[36] D.H. Broderick, B.C. Gates, AIChE J. 27 (1981) 663.
[37] M.L. Vrinat, L. de Mourgues, J. Chim. Phys. 79 (1982) 45.
[38] P.A. Rautanen, M.S. lylykangas, J.R. Aittamaa, A. Outi, I. Krause, Ind. Eng. Chem. Res. 41 (2002) 5966.